Experimental study of the droplet characteristics of a urea water solution spray through optical techniques.

G. Bracho[a], L. Postrioti[b], A. Moreno[a], G. Brizi[b]

[a] *CMT Motores Térmicos*
[b] *Università degli Studi di Perugia*

Abstract

The requirement of high-fidelity experimental data of microscopic properties of sprays motivates the continuous development of optical tools, since they are determinant in the understanding of atomization and evaporation process in a variety of multiphase flows. This work compares two optical techniques and an interferometry method for the measurement of the droplet size and velocity of a spray produced by a commercial Urea Water Solution (UWS) injector operating in high temperature cross flow. The adequate dosing and mixing of the injected UWS with the hot cross flow gasses is fundamental for the proper functioning of the Selective Catalytic Reduction SCR system. The SCR system is employed in the elimination of nitrous oxides present in exhaust gases of an engine. The objective is to compare the techniques in order to obtain accurate and reliable data that can be used to validate computational fluid dynamics models and improve current exhaust geometries and mixers. The studied techniques are Phase Doppler Anemometry (PDA), High Resolution Laser Backlight Imaging (HRLBI) and High Speed Microscopic Imaging (HSMI). The PDA determines the properties of the spray, obtaining the diameter and velocity of droplets in the axis parallel to the injector's axis. With the HRLBI frames of 2040 x 2040 pixels were captured at different instants of the injection event, achieving a spatial resolution of 7 um/pixel, allowing the visualization of the smallest droplets present in the spray. With the HSMI videos of the spray using a fast camera and a microscopic lens were recorded at 150.000 fps to measure the diameter and the velocity of the droplets in 2 directions. The measurements were carried out at 3 different injection pressures and the results are compared to determine the limits and advantages of each technique. The droplet diameter obtained by the PDA tests is similar to the observed results in the HRLBI, whereas the

HSMI missed the smaller droplets. On the other hand the droplet velocity is in good concordance in the axis parallel to the axis of the injector, proving the HSMI a suitable technique to quantify the velocity of the droplets.

Keywords: PDA, Imaging, water, droplet morphology, droplet velocity, SCR

---

1. Introduction

In engineering there are several industrial applications where the injection of a fluid into a gaseous cross-flow is essential. To investigate the behaviour of the sprays under this condition, optical techniques have become an important tool to obtain reliable experimental data. The advances in the image processing methodologies and camera sensors allow the measurement of the smallest particles present in a spray with high accuracy. There are experimental and numerical studies applied to different ambient conditions and regimes of cross flow, specially focused in atomization of the spray and liquid jet breakup [1–5]. In those studies the optical techniques were the cornerstone for the data acquisition and validation of the simulations.

The Selective Catalytic Reduction (SCR) system is one of the industrial applications where the measurement of the spray microscopic prorperties is fundamental. This system is the most favored solution to boost the reduction of NOx emissions in engines, as is shown in the studies done by Triantafyllopoulos et al. [6], where the performance of the SCR system is proved under real driving emissions test conditions. For the reactions that occur inside the SCR system, a Urea Water Solution (UWS) dosing unit must be placed upstream, where the fluid is introduced into the high temperature gas flow. The injected UWS must evaporate and generate ammonia through the thermolysis and hydrolysis of the fluid.

The UWS should evaporate entirely before it reaches the catalyst with an homogeneous distribution and appropriate quantity [7, 8]. Therefore, rapid decomposition and uniform distribution of ammonia over the inlet section of the catalyst must be used as targets in the designs of the SCR systems and particularly of its injection and mixer sections.

The literature supports that significant efforts are directed towards understanding and improving the SCR systems, specifically in regards of the UWS spray characteristics, from the whole spray (liquid and vapor penetration and spreading angle) to the microscopic point of view (droplet velocity, shape and diameter). It has become of great importance to determine these properties due to the consequences of improper spray mixing and dosing, such as the formation of deposits that might partially block the injector and exhaust pipe affecting the engine efficiency.

In the work of Brizi et al [9] the UWS spray was studied under different chamber temperatures and fluid temperatures, finding that the fluid temperature has great influence over the spray and droplet formation. Lieber, Koch and Bauser [10] studied an air assisted UWS injector with high temperature coaxial flow, determining the velocity of the gas by approximating it to the velocity of the smallest droplets and predicting the turbulent dispersion of the droplets. Postrioti et al [11] proposed a viable alternative based on back-light imaging for diameter determination and validated the results against PDA. Kapusta et al [12] compared the behaviour of a commercial UWS injector using UWS and water analysing various spray characteristics such as the spray tip penetration, angle, static flow rate and droplet distribution. Liao et al [13] performed an investigation of the SCR wall impingement characterizing the droplet properties near the wall by means of PDA.

In this study the Phase Doppler Anemometry (PDA), High Resolution Laser Backlight Imaging(HRLBI) and High Speed Microscopic Visualization (HSMV) techniques are employed to characterize the UWS spray. The goal is to understand the advantages and the limitations of each technique and to discuss how they can complement each other in order to acquire reliable data that will serve as input for computational fluid dynamics models, to validate them and to improve the designs and performance of the dosing unit. The specific objective of this paper is to compare the three different techniques to measure droplet characteristics as diameter and velocity.

The manuscript is divided in four sections. After the introduction, the methodologies, equipment and techniques are described along with the image processing implemented. The results of each technique are presented and then compared and discussed. Finally, the conclusions obtained from this study are presented.

2. Methodology and Experimental Setup

The study of the microscopic properties of the UWS spray is a difficult task that is performed in conditions where a single technique might not be enough to obtain all the necessary data, so complementary techniques should be used to properly measure said properties. In order to accomplish this objective an experimental campaign was performed to study the microscopic properties of a Urea water solution (UWS) spray and compare different methodologies to quantify droplet diameter and velocity through optical and interferometry techniques.

Three techniques were implemented during the experimental campaign: Phase Doppler Anemometry (PDA), High Resolution Laser Backlight Imaging (HRLBI) and High Speed Microscopic Visualization (HSMV). In Figure 1 an image captured of the studied spray shows the location of the measurements performed for each technique.

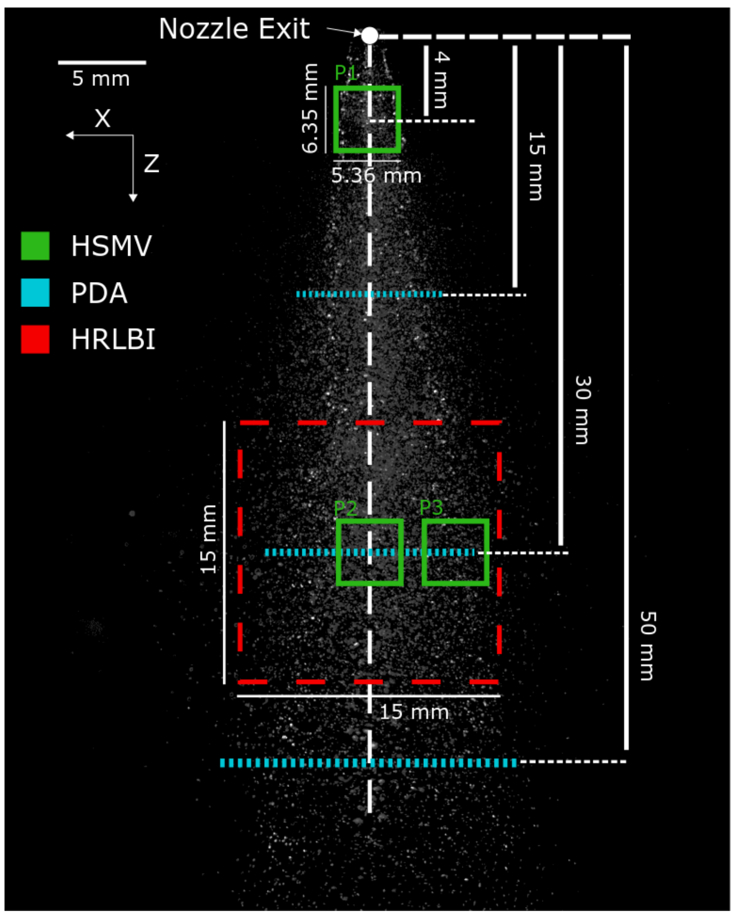

Figure 1: Image of the whole spray using Mie Scattering to show the location of the measurements performed with each technique.

The UWS was injected using a commercial Bosch three-hole, liquid cooled injector. The characteristics of the dosing module are summarized in table 1.

Table 1: Tested injector properties

Injector Properties	
Injector	Bosch Denoxtronic 5 dosing module
Injector type	Solenoid
Cooling	Liquid cooled
Number of holes	3
Hole diameter	135 μm

The test conditions used for the three techniques were the same and they are presented in table 2. The techniques and setups employed during the measurements are explained below. For the experiments and comparison of techniques, the selected work fluid was water and the differences with urea water solution are reported by Kapusta *et al* and Spiteri *et al*[12, 14].

Table 2: Tests Conditions

Test Conditions	
Injection Pressure	4-6-8 bar
Injection mass	3.90-4.80-5.40 mg/shot
Ambient Temperature	25°C
Injector Cooling Temperature	25°C
Energizing time	5 ms

2.1. Phase Doppler Anemometry (PDA)

The Phase Doppler Anemometry (PDA) is a common technique used to measure the diameter and velocity of spherical particles simultaneously and it has been widely employed for water and fuel sprays [15, 16]. The PDA system measures the light scattered by the particles that pass through a control volume formed by two incident laser beams coming from the emitter. The frequency of the scattered light measured in the receiver is proportional to the velocity of the particles, meanwhile the phase shift between the signals registered by two different detectors is proportional to the size of the particle

[17, 18]. Figure 2 shows a picture of the spray during the PDA tests and a scheme of the facility used for the measurements.

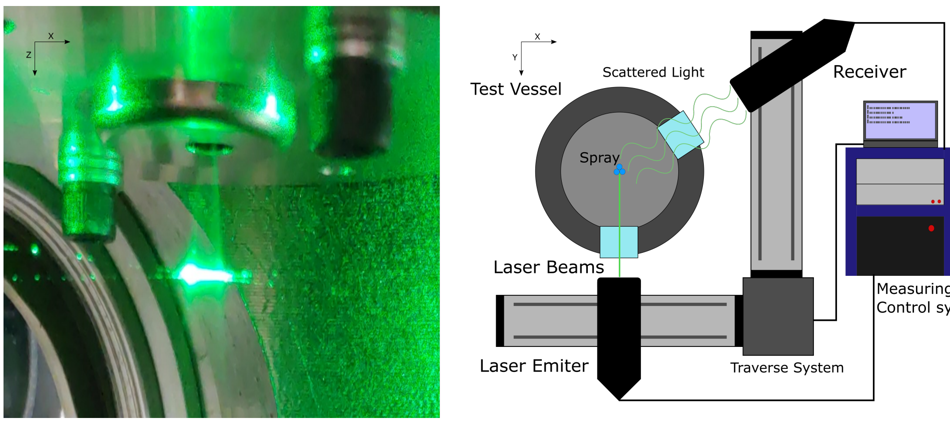

Figure 2: Phase Doppler Anemometry setup configuration.

In order to map the spray, measurements were performed at 15, 30 and 50 mm away from the nozzle exit (Z-axis) performing sweeps across the planes (X and Y directions), with a step of 1 mm between measurement points. To accomplish this, a 3-axis traverse system was used to position the measuring volume to the desired coordinates for the measurements. The technical specifications of the PDA system used in the measurements are described in table 3.

Table 3: Phase-Doppler Anemometer system specifications

Phase Doppler anemometer specifications	
Processor	Dantec BSA P80
Transmitter/Laser source	FlowLite 60 mm
Receiver	HiDense 112 mm
Beams diameter/spacing	2.2 mm/38 mm
Focal length (TX/RX)	400 mm / 310 mm
Velocity range	-15.85 to 47.49 m/s
Sizing range	1-400 µm

2.2. High Resolution Laser Backlight Imaging

Backlight imaging consists in placing the object to be measured, in the case of this study is the UWS spray, between a camera and a light source.

During the injection event, the spray blocks the light coming from the source and avoids the rays from reaching the camera. Therefore the spray or droplets appear as black pixels in the recorded image.

The high resolution laser backlight imaging setup is described in figure 3. It is composed by a charge-coupled device (CCD) camera (JAI TM-4200CL camera) with a resolution of 2048 x 2048 pixel. A 200 mm focal length lens (Nikon AF Micro-Nikkor 200 mm 1:4D) was mounted on the camera, allowing a field of view of 15 by 15 mm and a depth of field of ± 1.5 mm. The setup employed granted a spatial resolution of 7.3 µm per pixel. The back light source was a 532 nm pulsed New Wave Research Solo-PIV Nd-YAG laser that allowed to capture sharp images since the blurring effects are limited by the length of the laser pulse (<10 ns) and not the exposure time of the camera.

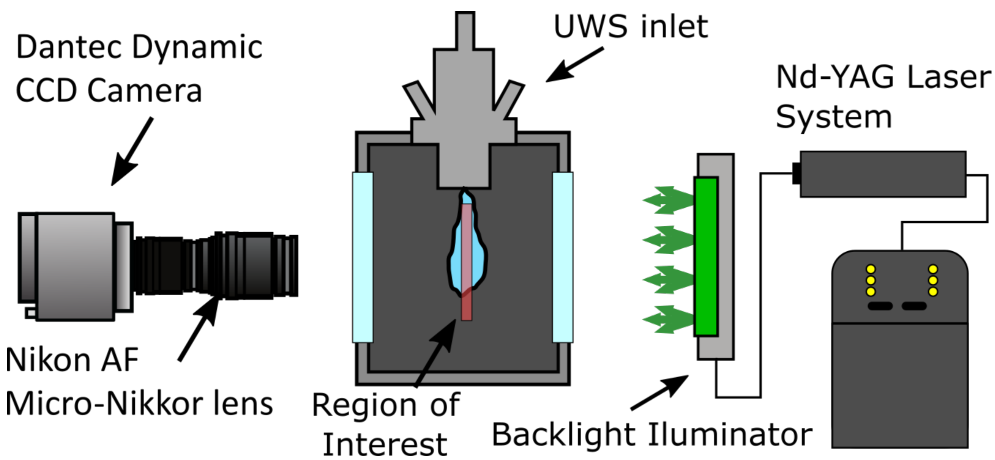

Figure 3: High Resolution Laser Backlight Imaging setup configuration.

The image acquisition was limited to one frame per injection event due to the operating frequency of the CCD Camera and the Nd-YAG laser, then to study the whole injection event different delays after the start of energizing have been set, from the beginning of the injection until the closing of the injector. In each one of these timings 200 images of the background and the spray were captured, allowing a robust population for the statistical analysis of the droplets.

2.3. High Speed Microscopic Imaging

Following the same principle of the High Resolution Laser Backlight Imaging, the High Speed Microscopic Visualization setup was composed of a camera (Photron Fastcam SA-X2) to capture the images at a recording speed of 150.000 frames per second, coupled with a K2 DistaMax microscopic lens to observe a region of 256 x 216 pixels with a spatial resolution of 24.8 µm per pixel. As a light source, an ultra-fast white light-emitting diode (LED), capable of short (10 ns), high-power pulses of light at high frequency, was implemented with a pulse duration of 200 ns and in front a diffuser and a Fresnel lens to create a homogeneous field of light in the region of interest. The main advantage of this technique is the determination of droplet velocity. Figure 4 shows a scheme of the optical setup implemented for this technique.

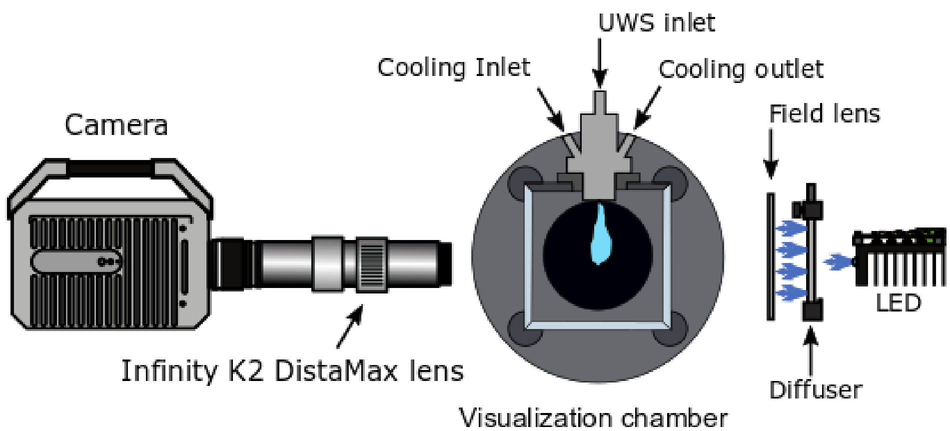

Figure 4: High Speed Microscopic Visualization setup configuration.

The high recording speed combined with the high frequency pulsed LED allowed to capture images of the whole injection event, granting the opportunity to visualize and track the droplets during their time of residence inside of the studied region of interest. For each of the tested conditions 10 repetitions were captured and processed.

2.4. Image Processing

2.4.1. High Resolution Backlight laser Imaging:

The image processing for this technique consists on several steps that allow to separate the droplets from the rest of the image. The first step is to subtract the background of each image to the corresponding spray image, this creates a grayscale image where the spray appears as greyscale dots in the image. Afterwards, the images are binarized to separate the background and out of focus spray from the droplets that will be measured. The chosen thresholding strategy is based on Yen´s approach. A detailed explanation of the Image processing and thresholding steps is available in the works of Postrioti et al [11] and Yen et al [19].

2.4.2. High Speed Microscopic Imaging:

The principle behind the image processing of both techniques is similar, beginning with the background subtraction. The first images before the start of injection are averaged and the resulting image is normalized and subtracted from each image with spray, returning greyscale images where droplets can be observed as dark pixels in each image.

The resulting images are binarized by applying a dynamic threshold that allows to filter the out of focus droplets, then the droplet information is extracted for each frame of the recording. The main difference with the previous technique is the ability to capture the whole injection event by recording images every 32 µs with the trade-off of less resolution. Therefore, the particles present in consecutive frames can be tracked and their position over time can be determined allowing the calculation of the two velocity components in the visualized plane.

A more comprehensive explanation of the image processing of microscopic DBI and droplet image processing can be seen in the works of Manin et al [20] and Blaisot and Yon [21] , and the detailed explanation of the droplet tracking is presented in the work of Payri et al [22].

3. Results

In this section the results obtained with each technique are presented individually. Then, a comparison of the three techniques is presented and discussed.

3.1. Phase Doppler Anemometry (PDA)

As explained in section 2.1, a PDA system was employed to determine the droplet diameter and velocity in the Z direction along several positions of the UWS spray. In figure 5 a schematic of the location of the measurement planes is shown, where the test points are located in these three planes at 15 mm, 30 mm and 50 mm from the nozzle exit.

The traverses analysed were those where a higher droplet count was found by performing preliminary measurements in each axis (X and Y), defining these as the centre of the plume in each measurement plane, which does not necessarily coincide with the injector axis. The measured positions in each traverse increased when the measurement plane was further away from the nozzle exit in order to capture the whole spray cone.

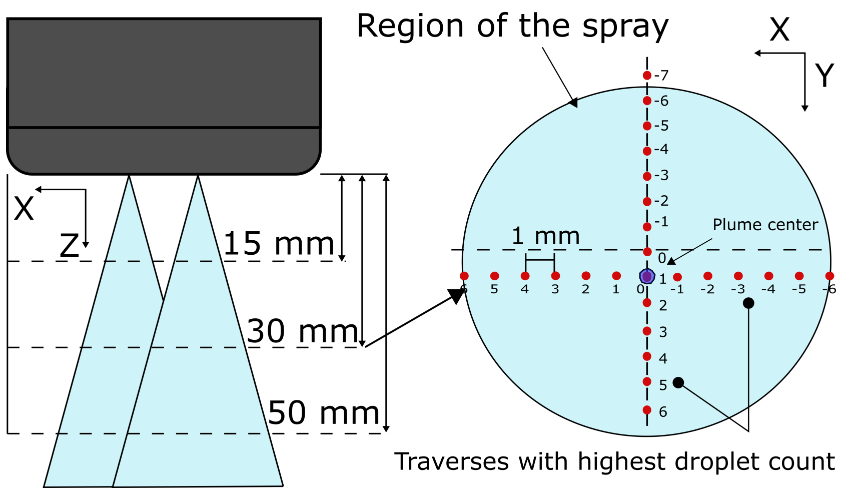

Figure 5: Studied planes and measured positions inside the plane 30 mm away from the nozzle exit.

Figures 6 and 7 show an example of the output from the PDA system in two position (Z = 15 and Z = 30), where it can be observed the evolution of the droplet diameter and velocity over time.

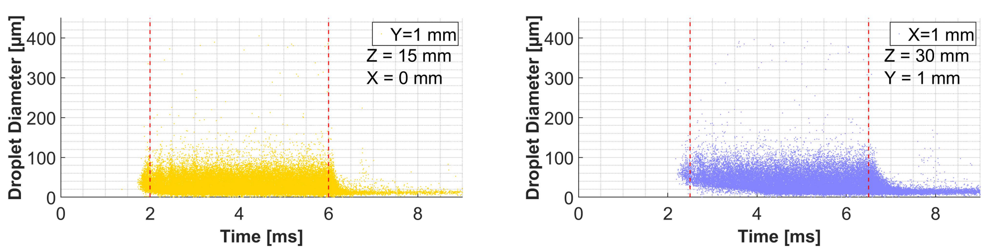

(a) Position Z = 15 mm, Y = 1 mm, X = 0 mm.

(b) Position Z = 30 mm, Y = 1 mm, X = 1 mm.

Figure 6: Droplet diameter acquisition over time

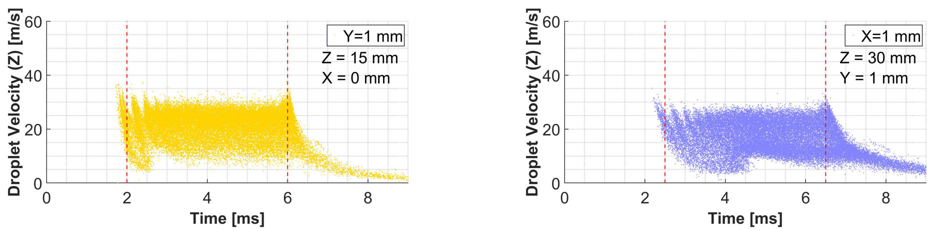

(a) Position Z = 15 mm, Y = 1 mm, X = 0 mm. (b) Position Z = 30 mm, Y = 1 mm, X = 1 mm.

Figure 7: Droplet Velocity acquisition over time.

To process the raw data obtained from the PDA system a time window was selected according to the measured position, where the injection event in its stabilized conditions (no influence of the needle opening or closing) takes place and is represented in figures 6 and 7 with the vertical dashed lines. With this information the properties of the spray in each traverse can be processed and summarized as shown in figures 8 and 9. They show the droplet count for each position in the traverse, the Sauter Mean Diameter (SMD), the droplet diameter probability density function (PDF) and the Cumulative Volume Fraction (CVF) curves for the three tested injection pressures.

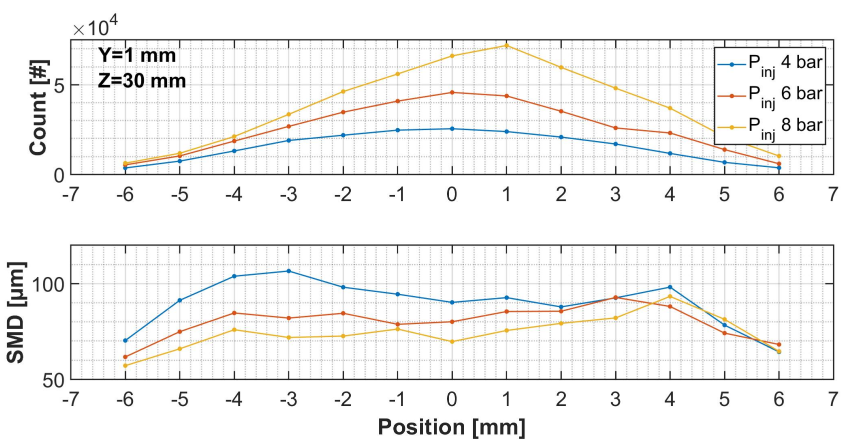

Figure 8: Droplet count and Sauter Mean Diameter (SMD) in the X traverse at Z = 30 mm and Y = 1 mm for the three tested injection pressures.

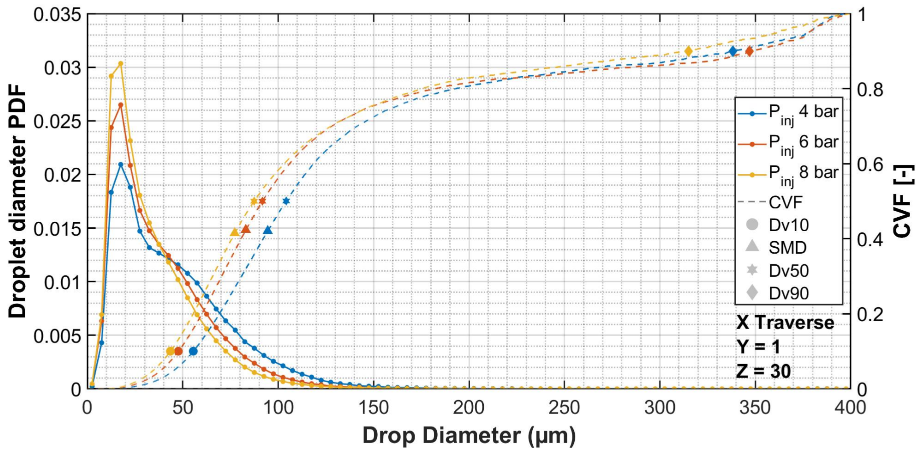

Figure 9: Droplet diameter Probability Density Function (PDF) and Cumulative Volume Fraction (CVF) curves in the X traverse at Z = 30 mm and Y = 1 mm three tested injection pressures.

The figure 8 shows how the droplet count increases significantly, producing finer droplets for higher injection pressures. This behaviour is directly reflected on the SMD, showing a decrease in its value for all measured positions.

Figure 9 presents the PDF curves for each tested injection pressure and in the left axis the CVF curves are presented simultaneously, where the location of the characteristic diameters Dv10, SMD, Dv50 and Dv90 are indicated with symbols. It is observed how for the injection pressure of 8 bar the amount of finer droplets is higher meanwhile for the lowest injection pressure there is a higher probability for droplets with diameter above 50 µm. The volume fraction is also affected by the injection pressure and it is observed as the cumulative volume fraction curves shift to the left for higher injection pressure. This is due to a better atomization of the spray generating a higher quantity of finer droplets and is also reflected in the characteristic diameters where the Dv10, SMD and Dv50 become smaller as the injection pressure is increased.

Figure 10 shows the velocity distributions of the recorded droplets at 30 mm from the nozzle exit, for all the injection pressures in the Z direction of the spray. The range of the velocity goes from 0 to 40 m/s and the distribution, having higher probability for faster droplets with higher injection pressures. Furthermore, a reduction of the probability for slower droplets(below

10 m/s) is observed as the injection pressure is increased.

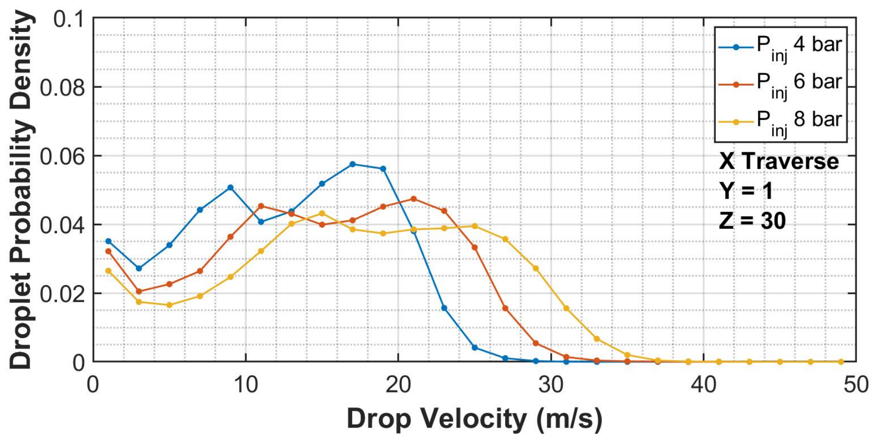

Figure 10: Velocity Probability Density function curves for the three tested injection pressures.

Figure 11 shows the droplet average velocity in each position over the X axis. For the lowest injection pressure the velocity is more uniform along all the measured locations of the spray, rounding the 12 m/s, but as the injection pressure is increased the velocity in all position increases.

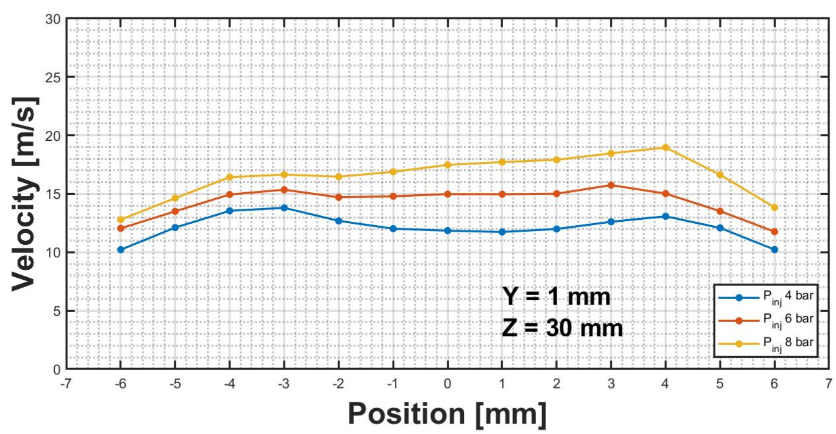

Figure 11: Droplet average velocity along the X traverse in Z = 30 mm and Y = 1 mm.

3.2. High Resolution Laser Backlight Imaging

With the following technique the droplet diameter values were calculated for different instants after start of energizing (ASOE) of the injector, capturing images with its centre located at 30 mm from the nozzle exit. Figure 12 shows an example of the images taken during the test at 2.5, 4.5 and 7.5 ms ASOE, where it is observed how the spray begins to appear inside the region of interest at 2.5 ms ASOE, then the developed spray is shown at 4.5 ms ASOE and the effects of closing of the injector can be seen at 7 ms ASOE.

In figure 13 the results of the image processing are presented. For each injection pressure the diameter probability density function and cumulative volume fraction is calculated. The results behave as expected and are in concordance with those found in the literature for similar studies for this kind of injector [9, 12]. As mentioned before, the increase in the injection pressure produces finer droplets, making the droplet distribution in these conditions have smaller diameter values.

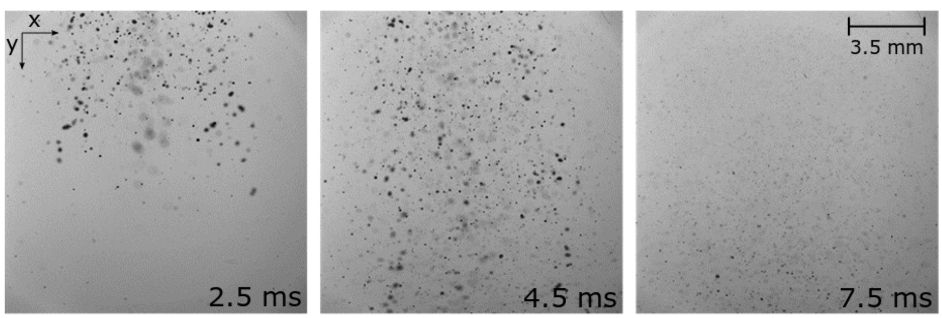

Figure 12: Images from the spray at 2.5, 4.5 and 7.5 ms obtained with the HRLBI technique

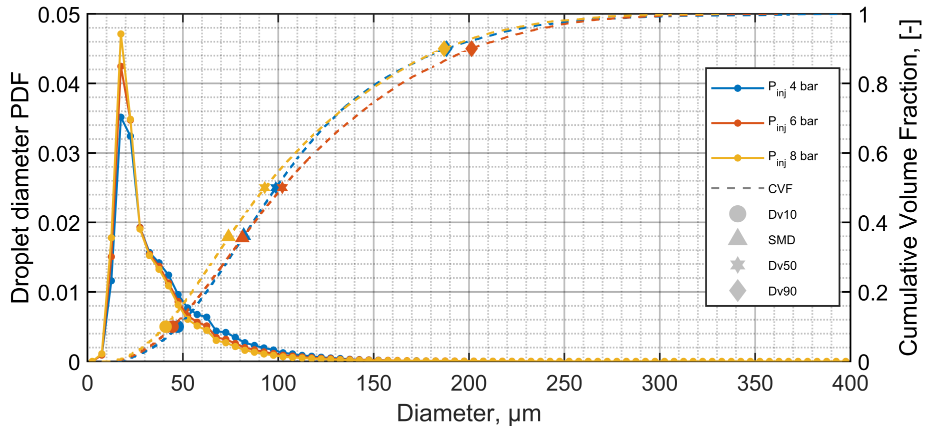

Figure 13: PDF and CVF curves for the three tested injection pressures.

The figure 14 shows the evolution of the Sauter mean diameter over time, showing similar values for all injection pressures during the injection event. Furthermore, two particular peaks at 2.5 ms and 7.5 ms can be observed. The first peak at 2.5 ms denotes the first packages of big droplets and ligaments due to the opening of the injector meanwhile at 7.5 ms there is a significant decrease in the value of the SMD due to the closing of the injector and an increase afterwards above of their mean value that can be attributed to the final bobbles and ligaments formed when the needle of the injector closes.

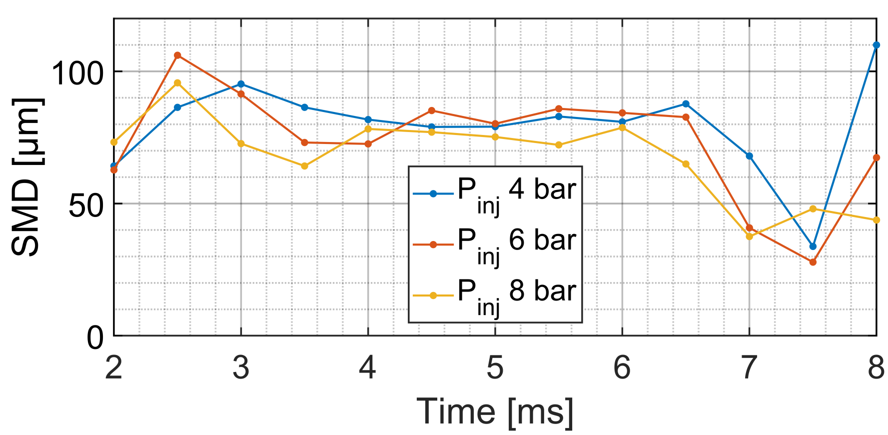

Figure 14: Sauter Mean Diameter evolution over time.

3.3. High Speed Microscopic Imaging

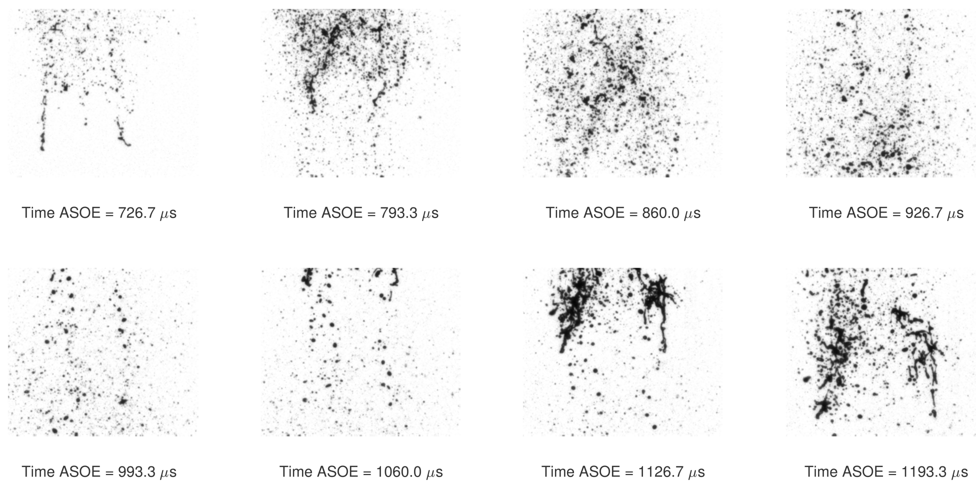

Figure 15: Images from the spray at different time steps obtained with the HSMI technique [23]

This technique is used to determine droplet diameter and velocity in the two components X and Z simultaneously. Figure 16 displays the results obtained from the high speed microscopic visualization technique, showing the corresponding probability density function curves and the cumulative volume fraction for each tested injection pressure at a distance of 30 mm from the nozzle exit on the spray axis. The injected spray presents similar characteristics in this position for the injection pressure of 6 and 8 bar, showing a higher probability of smaller droplets for the latter value, also observed in the CVF curves where droplets of lower diameter represent a higher portion of the total volume for the higher injection pressure.

Meanwhile at the injection pressure of 4 bar a lower amount of droplets below 50 µm are observed and there is higher probability for droplets above 100 µm to be encountered than for the 6 and 8 bar injection pressures. This is consistent with the worse atomization generated at 4 bar where more blobs and ligaments could be observed and is also reflected in the cumulative volume fraction curve. This technique detects that most of the volume of the droplets is concentrated in diameters above 150 microns.

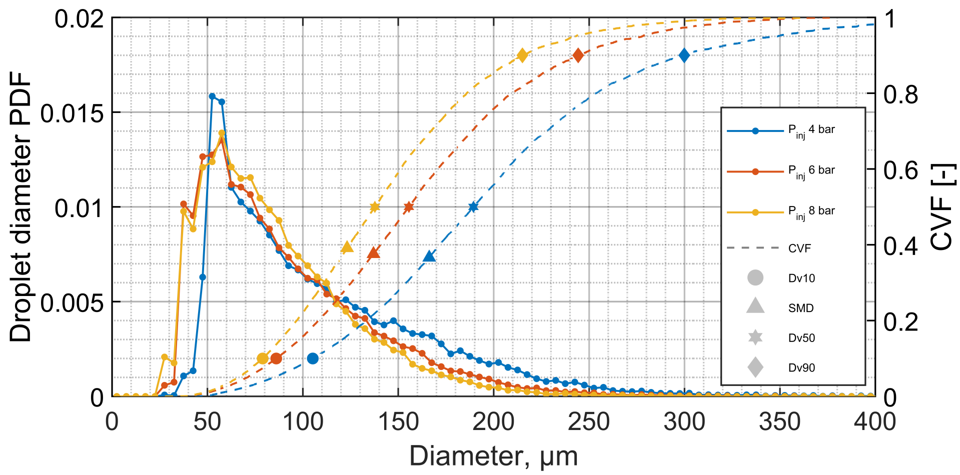

Figure 16: PDF and CVF curves for the three tested injection pressures.

Figures 17 and 18 show the probability density function curves for the velocity in the X and Z component of the spray respectively. The velocity of the droplets in the X direction is calculated following the methodology explained by Payri et al [22] (Note that the X direction is perpendicular to the spray axis). Results show that the velocity in the X direction is faster when the injection pressure is increased, and could be an indication of the tangential movement of the droplets due to a higher turbulence of the fluid as it exits the nozzle of the injector.

In the X direction the velocity has negative and positive values in an almost symmetrical way due to the spray opening in the radial direction, nevertheless there is a significant amount of droplets that only posses velocity in the Z component.

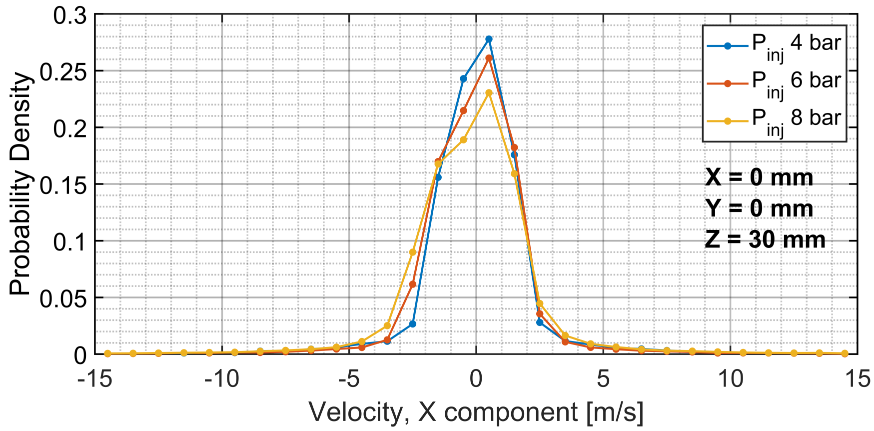

Figure 17: Droplet velocity distribution in the X direction 30 mm away from the nozzle exit.

As for the Z component of the velocity, the injection pressure plays an important role in the observed values as expected. Higher injection pressure causes a higher exit velocity of the fluid from the nozzle and it is reflected on the droplets velocity downstream.

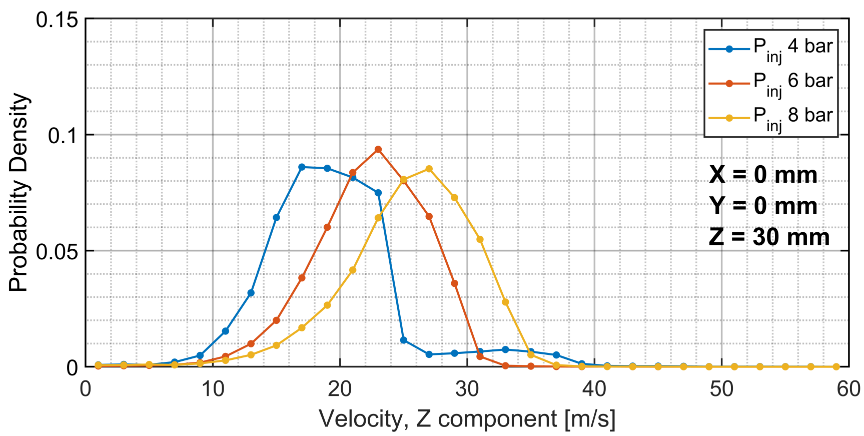

Figure 18: Droplet velocity distribution in the Z direction 30 mm away from the nozzle exit.

3.4. Comparison between techniques

In order to compare the data obtained from the three techniques, the focus will be set in the position 30 mm away from the nozzle exit on the spray axis. For this purpose, the corresponding position for PDA was analysed individually and the data obtained from the High Resolution Laser Backlight Imaging (HRLBI) was filtered to characterize only the droplets located inside a region of 4 by 4 mm surrounding the position, which is approximately the same window used for the High Speed Microscopic Visualization (HSMV). The results from this procedure are presented in figure 19.

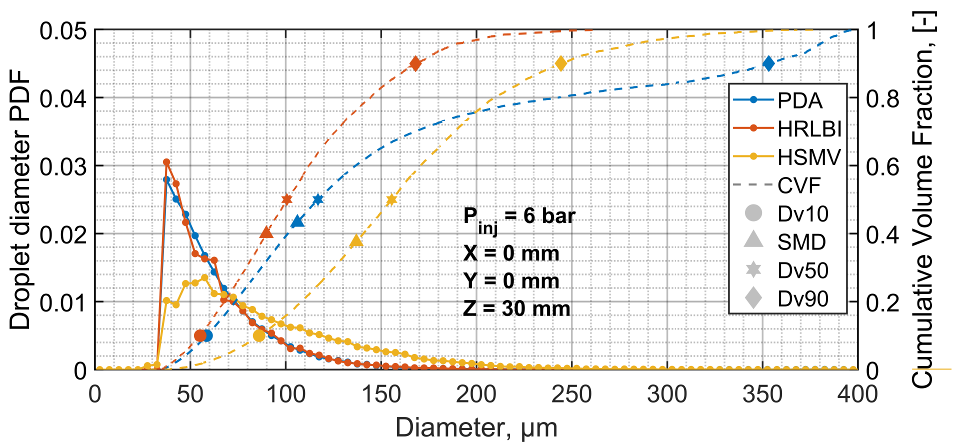

Figure 19: PDF and CVF curves for the three techniques at 30 mm from the nozzle exit with an injection pressure of 6 bar.

In the figure it is observed how the PDA and HRLBI data are in concordance, showing a range for droplet diameter and CVF curves that are very similar. The characteristic diameters also show similar values, except for Dv90 which is heavily affected by big droplets over 350 µm .

The main difference between the HSMV and the other techniques is observed in the lower probability for droplets in the range between 35 and 70 µm. This difference could be attributed to the criteria applied to keep the droplets during the image processing step, which required that the droplets remained in the focus plane for at least 4 consecutive frames for this technique.

The velocity in the Z direction obtained with the PDA and HSMV techniques in the position 30 mm away from the nozzle exit are compared in the range of diameters from 35 to 350 microns. Figure 20 shows a scatter of the droplet velocity versus its correspondent diameter where similar trends can be observed in both techniques.

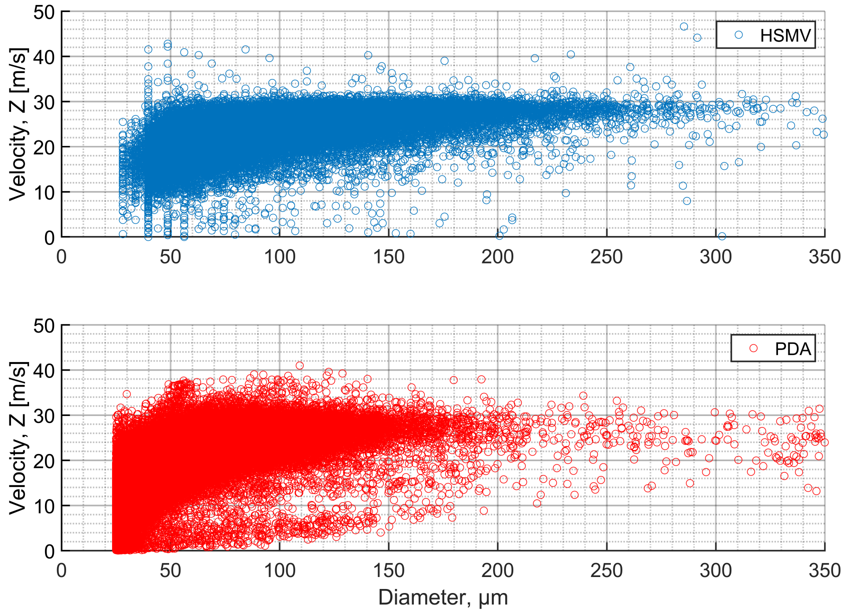

Figure 20: Droplet velocity versus diameter.

Smaller droplets have a wide range of velocities ranging from 0 m/s to 40 m/s, meanwhile as the diameter of the droplets increases most droplets travel at the same velocity, converging towards 30 m/s. This behaviour is observed with both techniques and an average velocity of the droplets for all injection pressures is presented in figure 21.

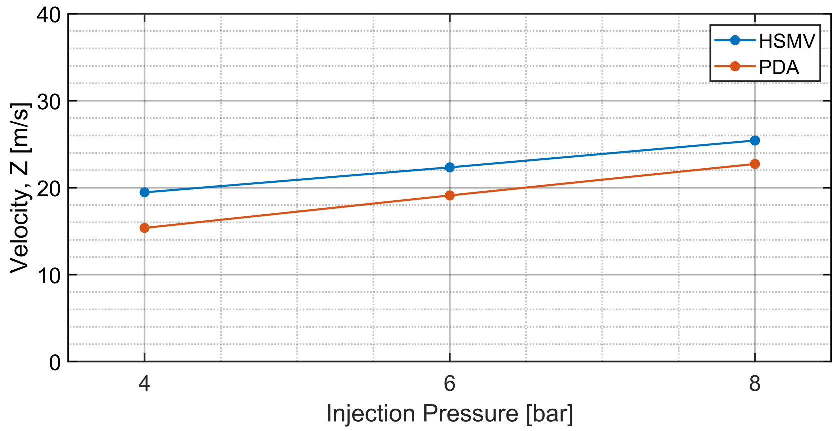

Figure 21: Droplet average velocity in Z direction for each tested injection pressure.

The figure shows that the average velocity increases almost linearly in the tested injection pressure range, showing a similar slope for both techniques and a difference of nearly 2 m/s between the averages of the measured velocity for each techniques in every tested injection pressure.

3.5. Discussion

Diameter distributions and droplet velocity are important parameters necessary to obtain a profitable design of the SCR system and also to validate computational fluid dynamics (CFD) models. The characterization of the droplets can vary depending on the experimental technique used. This section compares and analyze the similarities and differences of the three methods employed in the current study.

From one side, PDA has the most robust data acquisition, but it could become a challenge due to the necessary precision in the alignment needed in the equipment to measure accurately, especially for the complexity of the test chamber geometries used to reproduce existing SCR systems. Therefore, using visualization techniques such as the HRLBI and HSMV are viable options to capture the microscopic characteristics of the spray. These techniques acquire data faster, capturing relatively large areas of the spray in each position, meanwhile the PDA system can only make local measurements and require a high number of samples in each test point.

For the droplet diameter the HRLBI technique shows great concordance with the data obtained from the PDA, capturing a comparable range of droplet size and showing similar PDF and CVF curves for the same test conditions. Moreover, the optical techniques can identify liquid ligaments and blobs which are present in low pressure injector sprays and calculate an equivalent diameter for them.

On the other hand, the HSMV lacks the ability to detect droplets of small diameter which affects considerably the PDF and CVF curves of the spray and to obtain a better similarity with the results of the HRLBI and PDA improvements in the optical setup and a higher resolution have to be achieved.

As for the velocity of the droplets in the Z direction there is good agreement between the PDA and the HSMV, showing that the trend of the captured droplets velocity and the average velocity is similar in both techniques. The HSMV also allows the detection of the velocity in the X direction of the spray.

Overall the advantages of the image-based techniques can be summarized as:

– Time effort is low compared to the PDA measurement (local measurement, several thousand valid samples required in each position).

– Complex optical access to a complex domain, with an accurate positioning device required for the PDA probes.

– PDA cannot measure blobs diameter (Dual PDA can measure diameter over two orthogonal planes), which are skipped particularly from sizing measurement with a standard PDA system. Typically, with low pressure sprays (producing a lot of relatively large, blobs) the PDA validation for velocity measurement can be very high (>90%), while for sizing measurement it can hardly approach 60-70%.

All visualization techniques show great promise in the detection and characterization of the microscopic properties of the spray and there is still room for improvement in the image processing and the optical setups to close the gaps between these techniques and the PDA.

4. Conclusions

In the presented article, the measurements of a urea water solution injector spray using different techniques to characterize its microscopic properties under different injection pressure are presented.

The tests were performed using a Phase Doppler Anemometry (PDA) system and two optical techniques, the High Resolution Laser Backlight Imaging (HRLBI) and the High Speed microscopic visualization (HSMV).

The PDA measurements were carried out in 3 different planes at 15, 30 and 50 mm from the nozzle exit in the Z direction, where traverses along the X and Y direction were performed to measure the droplet diameter and velocity in each position.

The HRLBI technique consisted in capturing images at different times from the start of energizing of the injector using a fast shutter CCD camera and as a light source a pulsed Nd-YAG laser coupled with a backlight diffuser. Meanwhile, the HSMV used a High speed CMOS camera coupled with a microscopic lens to record the whole injection event at a recording speed of 150.000 frames per second, using as a light source a short duration pulse LED that allowed to capture sharp images.

The main results of the experiments are:

- PDA measurements showed a higher amount of droplets towards the centre of the spray and the quantity of droplets increased significantly with the injection pressure. The characteristic diameters such as the Sauter mean diameter becomes smaller with higher injection pressure.
- The Probability Density Function (PDF) curves show a higher probability of smaller droplets as the injection pressure is higher, showing in the cumulative volume fraction curve that at 8 bar a higher portion of the volume is contained in smaller droplets compared with the curve of 4 bar.
- The velocity distribution of the droplets is similar in shape, obtaining higher velocity values as the injection pressure is increased. Their velocity remains similar in different points of the traverse, increasing slightly towards the centre of the spray.
- The HRLBI technique showed similar PDF and CVF curves for the 3 injection pressures, with higher probability of encountering smaller diameter droplets as the injection pressure increased.
- During the time steps of the acquired data it can be highlighted how the opening and closing of the injector have an important effect over the characteristic diameters of the spray, observing an increase of the

SMD during the opening and a drastic reduction of it during the closing, followed by another increase caused by the blobs produced by the closing of the needle.

- The HSMV technique failed to capture smaller droplets which had a noticeable effect over the PDF and CVF curves.

- The droplet velocity was measured for the Z and X component of the spray with the HSMV technique. The Z component was compared to the velocity obtained from the PDA system which showed a good level of agreement between techniques for all injection pressures.

Overall, optical techniques such as the ones presented in this paper offer a good alternative to characterize UWS spray microscopic properties under conditions where the interferometry techniques might be difficult or impossible to apply properly.

5. Acknowledgments

The equipment used for the experiments was financially supported by MEMORIA IDIFEDER/2018/037 "*Diagnóstico óptico a alta velocidad para el estudio de procesos termo-fluidodinámicos en sistemas de inyección*" from Generalitat Valenciana.

The Dipartimento di Ingegneria – University of Perugia is also acknowledged for the support to experimental activities with Ricerca di Base - 2019 Program.

The author A. Moreno thanks the Universitat Politècnica de València for his predoctoral contract (FPI-2018-S2-13), which is included within the framework of Programa de Apoyo para la Investigación y Desarrollo (PAID).

References

[1] F. Xiao, Z. G. Wang, M. B. Sun, J. H. Liang, N. Liu, Large eddy simulation of liquid jet primary breakup in supersonic air crossflow, International Journal of Multiphase Flow 87 (2016) 229–240. URL: `http://dx.doi.org/10.1016/j.ijmultiphaseflow.2016.08.008`. doi:`10.1016/j.ijmultiphaseflow.2016.08.008`.

[2] X. Li, M. C. Soteriou, Detailed numerical simulation of liquid jet atomization in crossflow of increasing density, International Journal of Multiphase Flow 104 (2018) 214–232. URL: https://doi.org/10.1016/j.ijmultiphaseflow.2018.02.016. doi:10.1016/j.ijmultiphaseflow.2018.02.016.

[3] A. Sinha, R. Surya Prakash, A. Madan Mohan, R. V. Ravikrishna, Airblast spray in crossflow - structure, trajectory and droplet sizing, International Journal of Multiphase Flow 72 (2015) 97–111. URL: http://dx.doi.org/10.1016/j.ijmultiphaseflow.2015.02.008. doi:10.1016/j.ijmultiphaseflow.2015.02.008.

[4] P. Dong, B. Lu, S. Gong, D. Cheng, Experimental study of submerged gas jets in liquid cross flow, Experimental Thermal and Fluid Science 112 (2020) 109998. URL: https://doi.org/10.1016/j.expthermflusci.2019.109998. doi:10.1016/j.expthermflusci.2019.109998.

[5] V. Sharma, V. Eswaran, D. Chakraborty, Effect of fuel-jet injection angle variation on the overall performance of a SCRAMJET engine, Aerospace Science and Technology 100 (2020) 105786. URL: https://doi.org/10.1016/j.ast.2020.105786. doi:10.1016/j.ast.2020.105786.

[6] G. Triantafyllopoulos, D. Katsaounis, D. Karamitros, L. Ntziachristos, Z. Samaras, Experimental assessment of the potential to decrease diesel NOxemissions beyond minimum requirements for Euro 6 Real Drive Emissions (RDE) compliance, Science of the Total Environment 618 (2018) 1400–1407. URL: https://doi.org/10.1016/j.scitotenv.2017.09.274. doi:10.1016/j.scitotenv.2017.09.274.

[7] G. Zheng, Development of Air-Assisted Urea Injection Systems for Medium Duty Trucks, SAE Technical Papers 2017-Septe (2017). doi:10.4271/2017-24-0112.

[8] J. Oh, K. Lee, Spray characteristics of a urea solution injector and optimal mixer location to improve droplet uniformity and NOx conversion efficiency for selective catalytic reduction, Fuel 119 (2014) 90–97. URL: http://dx.doi.org/10.1016/j.fuel.2013.11.032. doi:10.1016/j.fuel.2013.11.032.

[9] G. Brizi, L. Postrioti, N. van Vuuren, Experimental analysis of SCR spray evolution and sizing in high-temperature and flash boiling conditions, SAE International Journal of Fuels and Lubricants 12 (2019) 87–107. doi:10.4271/04-12-02-0006.

[10] C. Lieber, R. Koch, H.-j. Bauer, Microscopic Imaging Spray Diagnostics under High Temperature Conditions : Application to Urea – Water Sprays, Applied sciences (2019). doi:10.3390/app9204403.

[11] L. Postrioti, G. Brizi, C. Ungaro, M. Mosser, F. Bianconi, A methodology to investigate the behaviour of urea-water sprays in high temperature air flow for SCR de-NOx applications, Fuel 150 (2015) 548–557. URL: http://dx.doi.org/10.1016/j.fuel.2015.02.067. doi:10.1016/j.fuel.2015.02.067.

[12] Ł. J. Kapusta, M. Sutkowski, R. Rogóż, M. Zommara, A. Teodorczyk, Characteristics of Water and Urea–Water Solution Sprays, Catalysts 9 (2019) 750. doi:10.3390/catal9090750.

[13] Y. Liao, R. Furrer, P. Dimopoulos Eggenschwiler, K. Boulouchos, Experimental investigation of the heat transfer characteristics of spray/wall interaction in diesel selective catalytic reduction systems, Fuel 190 (2017) 163–173. URL: http://dx.doi.org/10.1016/j.fuel.2016.11.035. doi:10.1016/j.fuel.2016.11.035.

[14] A. Spiteri, P. Dimopoulos Eggenschwiler, Experimental fluid dynamic investigation of urea-water sprays for diesel selective catalytic reduction-denox applications, Industrial and Engineering Chemistry Research 53 (2014) 3047–3055. doi:10.1021/ie404037h.

[15] F. Durst, G. Brenn, T. H. Xu, A review of the development and characteristics of planar phase-Doppler anemometry, Measurement Science and Technology 8 (1997) 1203–1221. doi:10.1088/0957-0233/8/11/002.

[16] L. Postrioti, S. Malaguti, M. Bosi, G. Buitoni, S. Piccinini, G. Bagli, Experimental and numerical characterization of a direct solenoid actuation injector for Diesel engine applications, Fuel 118 (2014) 316–328. URL: http://dx.doi.org/10.1016/j.fuel.2013.11.001. doi:10.1016/j.fuel.2013.11.001.

[17] H.-E. Albrecht, M. Borys, N. Damaschke, C. Tropea, Laser Doppler and Phase Doppler Measurement Techniques, 2003. doi:10.1007/978-3-662-05165-8.

[18] A. Coghe, G. E. Cossali, Quantitative optical techniques for dense sprays investigation: A survey, Optics and Lasers in Engineering 50 (2012) 46–56. URL: http://dx.doi.org/10.1016/j.optlaseng.2011.07.017. doi:10.1016/j.optlaseng.2011.07.017.

[19] J. C. Yen, F. J. Chang, S. Chang, A New Criterion for Automatic Multilevel Thresholding, IEEE Transactions on Image Processing 4 (1995) 370–378. doi:10.1109/83.366472.

[20] J. Manin, M. Bardi, L. M. Pickett, R. N. Dahms, J. C. Oefelein, Microscopic investigation of the atomization and mixing processes of diesel sprays injected into high pressure and temperature environments, Fuel 134 (2014) 531–543. URL: http://dx.doi.org/10.1016/j.fuel.2014.05.060. doi:10.1016/j.fuel.2014.05.060.

[21] J. B. Blaisot, J. Yon, Droplet size and morphology characterization for dense sprays by image processing: Application to the Diesel spray, Experiments in Fluids 39 (2005) 977–994. URL: http://link.springer.com/10.1007/s00348-005-0026-4http://link.springer.com/article/10.1007/s00348-005-0026-4. doi:10.1007/s00348-005-0026-4.

[22] R. Payri, G. Bracho, J. Gimeno, A. Moreno, Investigation of the urea-water solution atomization process in engine exhaust-like conditions, Experimental Thermal and Fluid Science 108 (2019) 75–84. URL: https://doi.org/10.1016/j.expthermflusci.2019.05.019. doi:10.1016/j.expthermflusci.2019.05.019.

[23] R. Payri, G. Bracho, J. Gimeno, A. Moreno, A Methodology for the hydraulic characterization of a Urea-Water Solution injector by means of Spray Momentum Measurement, ILASS - Europe 2019, 29th Conference on Liquid Atomization and Spray Systems (2019) 2–4.